

New insight into the low-energy ${}^9\text{He}$ spectrum

M.S. Golovkov,¹ L.V. Grigorenko,¹ A.S. Fomichev,¹ A.V. Gorshkov,¹ V.A. Gorshkov,¹
 S.A. Krupko,¹ Yu.Ts. Oganessian,¹ A.M. Rodin,¹ S.I. Sidorchuk,¹ R.S. Slepnev,¹ S.V. Stepanyanov,¹
 G.M. Ter-Akopian,¹ R. Wolski,^{1,2} A.A. Korshennikov,^{3,4} E.Yu. Nikolskii,^{3,4} V.A. Kuzmin,⁴
 B.G. Novatskii,⁴ D.N. Stepanov,⁴ S. Fortier,⁵ P. Roussel-Chomaz,⁶ and W. Mittig⁶

¹Flerov Laboratory of Nuclear Reactions, JINR, Dubna, RU-141980 Russia

²The Henryk Niewodniczański Institute of Nuclear Physics, Kraków, Poland

³RIKEN, Hirosawa 2-1, Wako, Saitama 351-0198, Japan

⁴RRC “The Kurchatov Institute”, Kurchatov sq. 1, 123182 Moscow, Russia

⁵Institut de Physique Nucleaire, IN2P3-CNRS, F-91406 Orsay, France

⁶GANIL, BP 5027, F-14076 Caen Cedex 5, France

(Dated: July 15, 2018. File: `he9-11.tex`)

The spectrum of ${}^9\text{He}$ was studied by means of the ${}^8\text{He}(d,p){}^9\text{He}$ reaction at a lab energy of 25 MeV/n and small center of mass (c.m.) angles. Energy and angular correlations were obtained for the ${}^9\text{He}$ decay products by complete kinematical reconstruction. The data do not show narrow states at ~ 1.3 and ~ 2.4 MeV reported before for ${}^9\text{He}$. The lowest resonant state of ${}^9\text{He}$ is found at about 2 MeV with a width of ~ 2 MeV and is identified as $1/2^-$. The observed angular correlation pattern is uniquely explained by the interference of the $1/2^-$ resonance with a virtual state $1/2^+$ (limit on the scattering length is obtained as $a > -20$ fm), and with the $5/2^+$ resonance at energy ≥ 4.2 MeV.

PACS numbers: 25.45.Hi, 24.50.+g, 24.70.+s, 27.20.+n

Introduction. — Since the first observation of ${}^9\text{He}$ in the experiment [1] it was studied in relatively small number of works compared to the neighbouring exotic neutron dripline nuclei. This can be connected, on one hand, to the facts that technical difficulty of the precision measurements rapidly grows with move away from the stability line. On the other hand, already in the first experiment (pion double charge exchange on the ${}^9\text{Be}$ nucleus [1]) several narrow resonances were observed above the ${}^8\text{He}+n$ threshold. This observation was confirmed in Ref. [2], where the ${}^9\text{Be}({}^{14}\text{C}, {}^{14}\text{O}){}^9\text{He}$ reaction was used, and now the experimental situation with the low-energy spectrum of ${}^9\text{He}$ is considered to be well established. A new rise of interest to ${}^9\text{He}$ was connected with the question of a possible $2s$ state location in the framework of the shell inversion problem in nuclei with large neutron excess. The recent experiment [3] was focused on the search for the virtual state in ${}^9\text{He}$. An upper limit on the scattering length $a < -10$ fm was established in this work. The properties of states in ${}^9\text{He}$ were inferred in [4] basing on studies of isobaric partners in ${}^9\text{Li}$. The available results are summarized in Table I.

Interpretation of the ${}^9\text{He}$ spectrum as provided in [1, 2] faces certain difficulties which were not unnoticed (e.g. Ref. [5]). Indeed, the ground $1/2^-$ state is expected to be single particle state with width estimated as $0.8 - 1.3$ MeV at $E = 1.27$ MeV for typical channel radii $3 - 6$ fm. This requires spectroscopic factor $S \sim 0.1$ which contradicts single particle character of the state. F. Barker in Ref. [5] concludes on this point that “some configuration mixing in either the ${}^9\text{He}(1/2^-)$ or ${}^8\text{He}(0^+)$ state or both is possible, but is unlikely to be large enough to reduce the calculated width to the experimental value”. The next, presumably $3/2^-$ state, should be a compli-

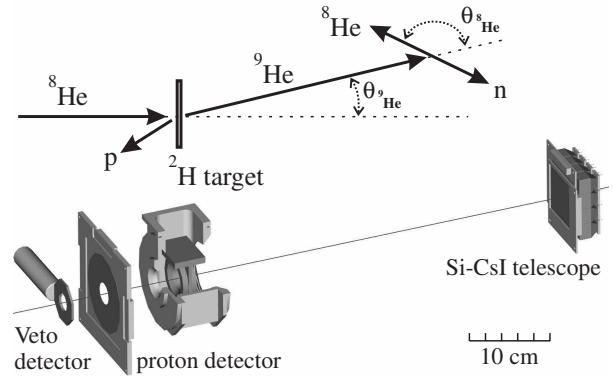


FIG. 1: Experimental setup, angles, and momenta.

cated particle-hole excitation as $p_{3/2}$ subshell is occupied. However, a much larger spectroscopic factor $S \sim 0.3 - 0.4$ is required for its widths found in a range $2.0 - 2.6$ MeV.

Having in mind the mentioned problematic issues we decided to study the ${}^9\text{He}$ in the “classical” one-neutron transfer (d,p) reaction well populating single particle states. In contrast with the previous works complete kinematics studies were foreseen to reveal the low-energy s -wave mode. Following the experimental concept of [6, 7], where correlation studies of ${}^5\text{H}$ continuum were accomplished by means of the ${}^3\text{H}(t,p)$ transfer reaction, this work was performed in the so called “zero geometry”.

Experiment. — The experiment was done at the U-400M cyclotron of the Flerov Laboratory of Nuclear Reactions, JINR (Dubna, Russia). A 34 MeV/nucleon ${}^{11}\text{B}$ primary beam delivered by the cyclotron hit a 370 mg/cm² Be production target. The modified AC-CULINNA fragment separator [8] was used to produce a

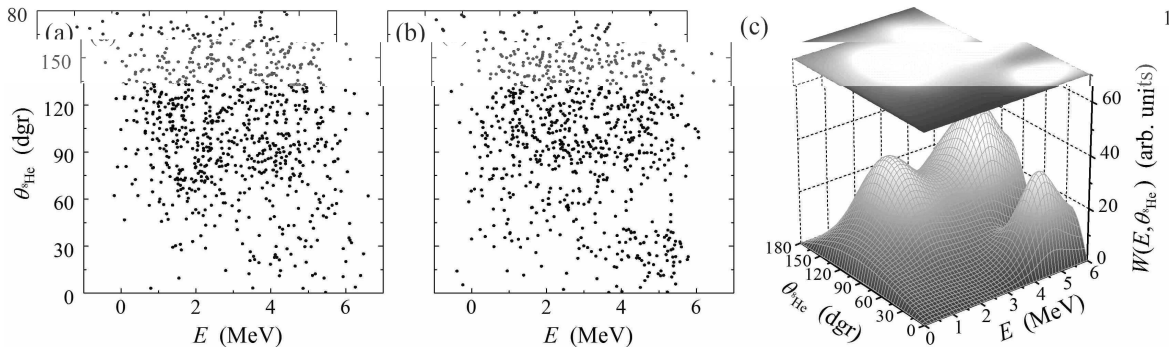


FIG. 2: (a) Experimental data on the $\{E, \theta_{\text{He}}\}$ plane. (b) MC simulation [with the same statistics as (a)] using the input shown in panel (c). (c) Theoretically reconstructed distribution with parameter set 1 from Table II. Hereafter, the ${}^9\text{He}$ energy E (missing mass) is given relative to the ${}^8\text{He}+n$ breakup threshold.

${}^8\text{He}$ secondary beam with a typical intensity of $2 \times 10^4 \text{ s}^{-1}$. The beam was focused on a cryogenic target [9] filled with deuterium at 1020 mPa pressure and cooled down to 25 K. The 4 mm thick target cell was supplied with 6 μm stainless steel windows, 30 mm in diameter.

Experimental setup and kinematical diagram for the ${}^2\text{H}({}^8\text{He}, p){}^9\text{He}$ reaction are shown in Fig. 1. Slow protons escaping from the target in the backward direction hit an annular 300 μm silicon detector with an active area of the outer and inner diameters of 82 mm and 32 mm, respectively, and a 28 mm central hole. The detector was installed 100 mm upstream of the target. It was segmented in 16 rings on one side and 16 sectors on the other side providing a good position resolution. The detection threshold for the protons (~ 1.2 MeV) corresponded to a ~ 5.5 MeV cutoff in the missing mass of ${}^9\text{He}$. We did not use here particle identification because, due to the kinematical constraints of the ${}^8\text{He}+{}^2\text{H}$ collisions, only protons can be emitted in the backward direction. The main cause of the background was due to evaporation protons originating from the interaction of ${}^8\text{He}$ beam with the material of target windows. This background was almost completely suppressed by the coincidence with ${}^8\text{He}$. The detection of such coincidences fixed the complete kinematics for the experiment.

Energy-momentum conservation was used for cleaning the spectra. Finally the comparison with an empty target run has shown that only $\sim 2\%$ events can be treated as a background.

The ${}^8\text{He}$ nuclei resulting from the ${}^9\text{He}$ decay, focused in narrow angular cone relative to the beam direction, were detected by a Si-CsI telescope mounted in air just behind the exit window of the scattering chamber. The 82 mm diameter exit window was closed by a 125 μm capton foil. The Si-CsI telescope consisted of two 1 mm thick silicon detectors and 16 CsI crystals with photodiode readouts. The 6×6 cm Si detectors were segmented in 32 strips both in horizontal and vertical directions, providing position resolution and particle identification by the $\Delta E-E$ method (together with following thick CsI detector). Sixteen $1.5 \times 2 \times 2$ cm CsI crystals were arranged as a 4×4 wall just behind the Si detectors. A 2% energy resolution of the CsI detectors allowed particle identification even for $Z = 1$ nuclei. The distance between the target and the telescope (50 cm) was sufficient to provide a good efficiency for the detection of the ${}^8\text{He}$ nuclei in coincidence with protons in the whole range of accessible ${}^9\text{He}$ energies. To eliminate signals in the proton telescope coming from the beam halo a veto detector was installed upstream the proton telescope. The energy of the ${}^8\text{He}$ beam in the middle of the target was ~ 25 MeV/nucleon. Energy spread of the beam, angular divergence, and position spread on the target were 8.5%, 0.23° , and about 5.4 mm respectively. A set of beam detectors was installed upstream of the veto (not shown in the Fig. 1). The beam energy was measured by two time-of-flight plastic scintillators with a 785 cm base. The overall time resolution was 0.8 ns. Beam tracking was made by two multiwire proportional chambers installed 26 and 80 cm upstream of the target. Each chamber had two perpendicular planes of wires with a 1.25 mm pitch. Energy resolution was estimated by Monte-Carlo (MC) code taking into account all experimental details. It was found to be 0.8 MeV (FWHM) for the ${}^9\text{He}$ missing mass.

Qualitative considerations. — Data obtained in the

TABLE I: Experimental positions of states in ${}^9\text{He}$ relative to the ${}^8\text{He}+n$ threshold (energies and widths are given in MeV).

Ref.	$1/2^+$		$1/2^-$		$3/2^-$		$5/2^+$	
	a (fm)	E	Γ	E	Γ	E	Γ	
[1]		1.13(10)	small ^b	2.3	small ^b	4.9		
[2]		1.27(10)	0.1(0.6)	2.42(10)	0.7(2)	4.3	small	
[3]	< -10							
[4] ^a		1.1		2.2		4.0		
Our	> -20	2.0(0.2)	2			≥ 4.2	> 1	

^aInferred from isobaric symmetry.

^bObserved peak width is smaller than the declared resolution.

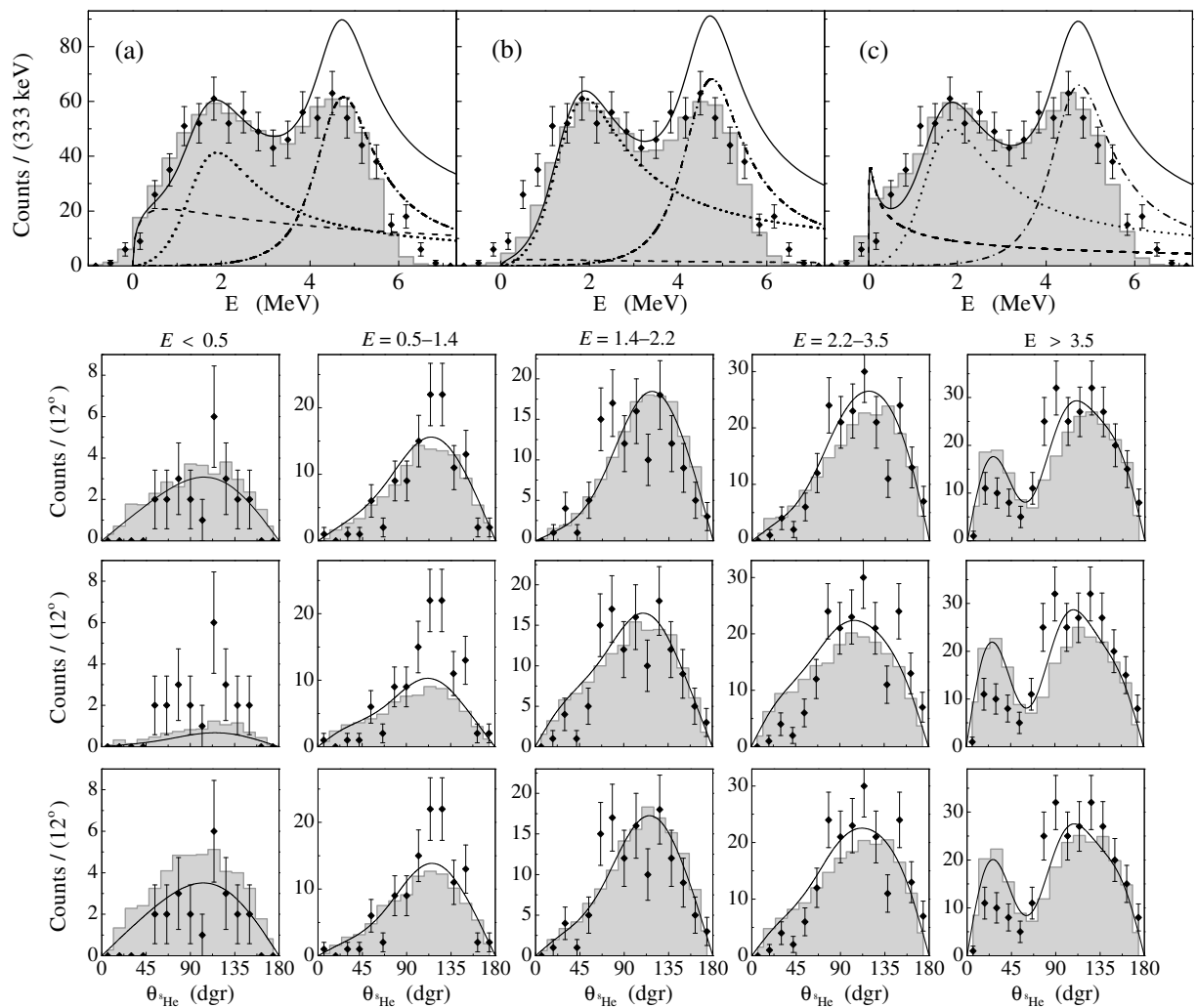


FIG. 3: Inclusive energy spectrum for the data of Fig. 2a is shown by diamonds. Theoretical curves in panels (a), (b) and (c) corresponds to parameter sets 1, 2, and 3 from Table II. Solid line is total result, while dashed, dotted and dash-dotted curves stand for contributions of $1/2^+$, $1/2^-$, and $5/2^+$ states. Gray histogram shows the results of MC simulation. The angular distributions for certain energy bins corresponding to panels (a), (b), and (c) are show in second, third and fourth rows.

experiment are shown in Figs. 2 and 3. The total number of counts corresponds to cross section of ~ 7 mb/sr. This value is consistent with the direct one-neutron transfer reaction mechanism at forward angles.

The narrow states known from the literature do not show up in the data. Instead, we get two broad peaks at about 2 and 4.5 MeV. Near the threshold the ${}^9\text{He}$ spectrum exhibits behavior (although distorted by the finite energy resolution of the experiment) which is more consistent with s -wave ($\sigma \sim \sqrt{E}$) rather than p -wave ($\sigma \sim E^{3/2}$). This is an indication for a possible virtual state in ${}^9\text{He}$.

An important feature of the data is a prominent forward-backward asymmetry with ${}^8\text{He}$ flying preferably in the backward direction in the ${}^9\text{He}$ c.m. system. This is not feasible if the narrow (means long-living) states of the ${}^9\text{He}$ are formed. To describe such an asymmetry the interference of opposite parity states is unavoidable. As

far as asymmetry is observed even at very low energy, the s - p interference is compulsory. Such an interference can provide only a very smooth distribution described by the first order polynomial [Eq. (2) and Fig. 3, $E < 2.2$ MeV]. Since above 3 MeV the character of the distribution changes to a higher polynomial, but asymmetry does not disappear, the p - d interference is also needed. This defines the minimal set of states as s , p , and d .

Theoretical model. — In the zero geometry approach the resonant states of interest are identified by the observation of recoil particle (here proton) at zero (in reality small, $3^\circ \leq \theta_p(\text{c.m.}) \leq 7^\circ$) angle. This means that the angular momentum transferred to the studied system should have zero projection on the axis of the momentum transfer. As a result we get a complete (strong) alignment for states with $J > 1/2$ in the produced system. In the ${}^9\text{He}$ case only the magnetic substates with $M = \pm 1/2$ should be populated for $J^\pi = 5/2^+$, $3/2^-$,

and $3/2^+$ states. This strongly reduces possible ambiguity in the analysis of correlation patterns. E.g. in the case of zero spin particles the zero geometry experiments give very clean pictures with angular distributions described by pure Legendre polynomial $|P_l^0|^2$. The situation in the case of nonzero spin particles involved is more complicated (see detailed discussion in Ref. [7]), and diverse correlation patterns are possible.

We have found that the observed experimental picture (Figs. 2, 3) can be well explained in a simple model involving only three low-lying states: $1/2^+$, $1/2^-$, and $5/2^+$. The inelastic cross in the DWBA ansatz is written as

$$\frac{d\sigma(\Omega_{\text{He}})}{dE d\Omega_{\text{sHe}}} \sim \frac{v_f}{v_i} \sqrt{E} \sum_{MM_S} \left| \sum_J \langle \Psi_f^{JMM_S} | V | \Psi_i \rangle \right|^2 \quad (1)$$

$$= \frac{v_f}{v_i} \sum_{MM_S} \sum_{JJ'} \sum_{M_l M_l'} \rho_{JM}^{J'M'} C_{VM_l SM_S}^{J'M'} C_{VM_l SM_S}^{JM} Y_{lM_l}^* Y_{lM_l}.$$

For the density matrix the generic symmetries are

$$\rho_{JM}^{J'M'} = (\rho_{J'M'}^{JM})^* \quad ; \quad \rho_{JM}^{J'M'} = (-)^{M+M'} \rho_{J-M}^{J-M'},$$

and properties specific to coordinate choice (spirality representation) and setup (zero geometry) are

$$\rho_{JM}^{J'M'} \sim \delta_{M,M'} (\delta_{M,1/2} + \delta_{M,-1/2}).$$

For the density matrix parametrization we use the following model for the transition matrix. The wave function (WF) Ψ_f is calculated in the l -dependent square well (with depth parameters V_l). The well radius is taken $r_0 = 3$ fm, which is consistent with typical R-matrix phenomenology $1.4A^{1/3}$. The energy dependence of the velocities v_i, v_f (in the incoming ${}^8\text{He}$ - d and outgoing ${}^9\text{He}$ - p channels) and WF Ψ_i is neglected for our range of ${}^9\text{He}$ energies. The term $V |\Psi_i\rangle$, describing the reaction mechanism, is approximated by radial θ -function:

$$V |\Psi_i\rangle \rightarrow C_l r^{-1} \theta(r_0 - r) [Y_l(\hat{r}) \otimes \chi_S]_{JM},$$

where C_l is (complex) coefficient defined by the reaction mechanism. For $|\rho_{J\pm 1/2}^{J'\pm 1/2}|$ denoted as $A_{l\nu}$ the cross section as a function of energy E and $x = \cos(\theta_{\text{sHe}})$ is

$$\frac{d\sigma(\Omega_{\text{He}})}{dE dx} \sim \frac{1}{\sqrt{E}} \left[4A_{00} + 4A_{11} + 3(1 - 2x^2 + 5x^4)A_{22} \right. \\ \left. + 8x \cos(\phi_{10})A_{10} + 4\sqrt{3}x(5x^2 - 3) \cos(\phi_{12})A_{12} \right]. \quad (2)$$

$$A_{l\nu} = |A_{l\nu}| |A_l|, \quad A_l = C_l N_l(E) e^{i\delta_l(E)} \int_0^{r_0} dr j_l(q_l r),$$

$$q_l = \sqrt{2M(E - V_l)}, \quad \phi_{l\nu}(E) = \phi_{l\nu}^{(0)} + \delta_{l\nu}(E) - \delta_l(E),$$

where N_l is defined by matching condition on the well boundary for internal function $j_l(q_l r)$. The three coefficients C_l give rise to the two phases $\phi_{10}^{(0)}$ and $\phi_{12}^{(0)}$.

Positions and widths of the states are fixed by the three parameters V_l . Their relative contributions to the inclusive energy spectrum (Fig. 3a-c) are fixed by the three

parameters $|C_l|$. The phase $\phi_{10}^{(0)}$ is fixed by the angular distributions at low energy, where the contribution of the d -wave resonance is small. After that the phase $\phi_{12}^{(0)}$ was varied to fit the angular distributions at higher energies (Fig. 3, $E > 2.2$ MeV). So, the model does not have redundant parameters and the ambiguity of the theoretical interpretation is defined by the quality of the data.

We have found that the weight and interaction strength for the $1/2^+$ state can be varied in a relatively broad range, still providing a good description of data. The results of MC simulations of the experiment with different s -wave contributions are shown in Fig. 3a-c. The parameter sets of the model are given in Table II; sets 1 and 2 correspond to small scattering length ($a = -4$ fm) and different weights of s -wave (largest and lowest possible), set 3 has $a = -25$ fm and largest possible weight of s -wave. It can be seen that the agreement with the data deteriorates when the population of the s -wave continuum falls, say, below 15 – 25% of the p -wave. On the other hand the large negative scattering length has a drastic effect below 0.5 MeV. The energy resolution and the quality of the measured angular distributions are not sufficient to draw solid conclusions about the exact properties of the s -wave contribution. The situations with the large contribution of the s -wave cross section but with moderate scattering length (say $a > -20$ fm) seem to be more plausible. Measurements with better resolution are required to refine the properties of the $1/2^+$ continuum.

Position of the d -wave resonance is not well defined in our analysis of data due to the efficiency fall in the high-energy side of the spectrum. This can be well seen from the comparison of theoretical inputs and MC results in Fig. 3a-c. The lower limit for the resonance energy of 4.2 MeV is in a good agreement with the value 4.0 MeV found in [4]. A broader energy range measured for ${}^9\text{He}$ is needed to resolve the $5/2^+$ state completely and to make the angular distribution analysis more restrictive.

Discussion. — It should be noted that the interference of any other combination of s - p - d -wave states *can not* lead to the required forward-backward asymmetry in the whole energy range. The correlation terms [square brackets in Eq. (2)] are

$$\begin{aligned} [\dots] &= 2A_{00} + 2A_{11} + (1 + 3x^2)A_{22} + 4x \cos(\phi_{10})A_{10} \\ &\quad + 2\sqrt{2}(3x^2 - 1) \cos(\phi_{20})A_{20}, \\ [\dots] &= 4A_{00} + 2(1 + 3x^2)A_{11} + 3(1 - 2x^2 + 5x^4)A_{22}, \end{aligned}$$

TABLE II: Parameters of theoretical model used in the work. V_i values are in MeV, weight coefficients for different states are normalized to unity $\sum |C_i|^2 = 1$.

Set	$ C_0 ^2$	$ C_1 ^2$	V_0	V_1	V_2	$\phi_{10}^{(0)}$	$\phi_{12}^{(0)}$
1	0.26	0.35	-4.0	-20.7	-43.4	0.80π	-0.03 π
2	0.03	0.52	-4.0	-20.7	-43.4	0.85π	-0.02 π
3	0.12	0.43	-5.817	-20.7	-43.4	1.00π	-0.03 π

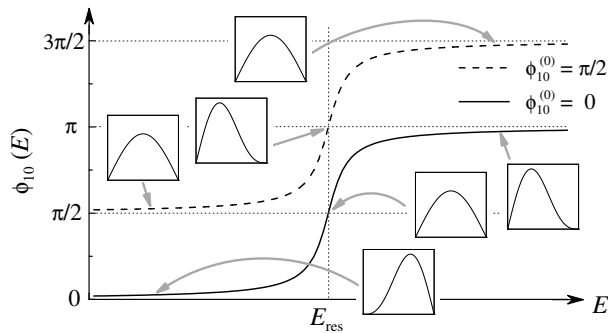


FIG. 4: Schematic illustration of possible behavior of angular distributions (shown by inserts for angles $\theta_{s_{\text{He}}}$ from 0° to 180°) due to $s_{1/2}$ - p_{12} interference around a narrow resonance for different phases $\phi_{10}^{(0)}$.

$$[\dots] = 2A_{00} + (1 + 3x^2)(A_{11} + A_{22}) + 2x(9x^2 - 5) \\ \times \cos(\phi_{12})A_{12} + 2\sqrt{2}(3x^2 - 1)\cos(\phi_{20})A_{20},$$

for $\{s_{1/2}, p_{1/2}, d_{3/2}\}$, $\{s_{1/2}, p_{3/2}, d_{5/2}\}$, and $\{s_{1/2}, p_{3/2}, d_{3/2}\}$ sets of states respectively. The asymmetric term ($\sim x$) is present here either for s - p interference only or for p - d only or for neither.

The angular distributions in energy bins (Fig. 3) provide a good indication that a *narrow* $p_{1/2}$ state is not populated in the reaction. Fig. 4 shows qualitatively what happens with angular distribution if there is a narrow resonance. The phase shift changes across the narrow resonance to a value close to π and the character of angular distribution should change drastically within this energy range. No trend of this kind is observed in Fig. 3. Phase shift for the *broad* $1/2^-$ state changes slowly and hardly achieves $\pi/2$ in our calculations. This allows to explain the smooth behaviour of asymmetry up to 3 MeV.

The existing experimental data can be regarded as not contradicting our results. In Refs. [1, 2] the narrow states were observed with low statistics (15–40 events/state). If the narrow states really exist they should be observable even at such a low counting rates. However, simulations show that if the cross section behavior is smooth, “statistically driven” narrow structures are quite probable in such a situation. A look at the data of Ref. [4] also shows that states (which should have analogues in ^9He) at 2.2 MeV and 4.0 MeV are absolutely evident in the data.

However, the presence of a narrow 1.1 MeV state is more likely not to contradict the data, rather than necessarily follow from these.

The idea that only the $1/2^-$ resonance state can be found in the low energy region not only looks natural, but also finds support in the recent theoretical studies. In Ref. [10], which deals with the whole chain of helium isotopes in continuum shell model, the $1/2^-$ state is located at 1.6 MeV above the $^8\text{He}+n$ threshold and the width is ~ 0.6 MeV indicating the dominant single particle component in the WF. The $3/2^-$ state is predicted to be at 6.6 MeV and relatively narrow (~ 2.5 MeV), what is natural for complicated particle-hole excitations.

Conclusions. — We would like to emphasize the following results of our study.

(i) Our data show two broad overlapping peaks (at 2 and at 4.5 MeV) in the ^9He spectrum. Statistics obtained in our experiment is about factor of 10 higher than in the previous works [1, 2]. Our resolution is sufficient to resolve narrow low-lying states. Even if a narrow $p_{1/2}$ is not resolved, the rapid change of phase around resonance energy should produce the change in the forward-backward asymmetry, which is also not seen in the data.

(ii) An essential contribution of the s -wave $1/2^+$ state is evident from the data. It is manifested in two ways: (a) Large forward-backward asymmetry at $E \leq 3$ MeV and (b) accumulation of counts around the threshold, which should not take place for typical cross section behavior for higher l -values. A limit $a > -20$ fm is obtained for the scattering length of this state.

(iii) The proposed spin assignment $\{s_{1/2}, p_{1/2}, d_{5/2}\}$ is unique, as no other reasonable set of low-lying states can provide the observed correlation pattern.

(iv) The experimental data are well described in a simple single-particle potential model, involving only basic theoretical assumptions about the reaction mechanism and the low-energy spectrum of ^9He . This supports the idea that ^8He (having closed $p_{3/2}$ subshell) presents a “good” core in the ^9He structure.

Acknowledgments. — This work was supported by the Russian Foundation for Basic Research grants 02-02-16550, 02-02-16174, 05-02-16404, and 05-02-17535 by the INTAS grantS 03-51-4496 and 03-54-6545. LVG acknowledge the financial support from the Royal Swedish Academy of Science and Russian Ministry of Industry and Science grant NS-1885.2003.2.

[1] K. Seth, *et al.*, Phys. Rev. Lett. **58**, 1930 (1987).
[2] H.G. Bohlen, *et al.*, Prog. Part. Nucl. Phys. **42**, 17 (1999).
[3] L. Chen, *et al.*, Phys. Lett. **B505**, 21 (2001).
[4] G.V. Rogachev, *et al.*, Phys. Rev. C **67**, 041603R (2003).
[5] F.C. Barker, Nucl. Phys. **A741**, 42 (2004).
[6] M. Golovkov, *et al.*, Phys. Rev. Lett. **93**, 262501 (2004).

[7] M. Golovkov, *et al.*, Phys. Rev. C **72**, 064612 (2005).
[8] A.M. Rodin, *et al.*, Nucl. Instr. Meth. **A** 391, 228 (1997).
[9] A.A. Yukhimchuk, *et al.*, Nucl. Instrum. Meth. **A** 513, 439 (2003).
[10] A. Volya and V. Zelevinsky, Phys. Rev. Lett. **94**, 052501 (2005).